ELSEVIER

Journal of Molecular Structure 378 (1996) 177–188

Journal of
MOLECULAR
STRUCTURE

Second harmonic generation in push–pull ethylenes: Influence of chirality and hydrogen bonding

K. Mohanalingam, M. Nethaji, Puspendu Kumar Das*

Department of Inorganic and Physical Chemistry, Indian Institute of Science, Bangalore 560 012, India

Received 4 September 1995; accepted 7 November 1995

Abstract

The effect of chiral substituents and hydrogen bonding functional groups on the microscopic and macroscopic second-order non-linearities in some donor–acceptor substituted ethylenes has been investigated. It appears that extensive intramolecular and intermolecular hydrogen bonding helps to improve both the microscopic hyperpolarizability (β) as well as the powder second harmonic generation (SHG) efficiency in these compounds. The substitution of the chiral α-methylbenzylamine donor guarantees a non-centrosymmetric structure. Cocrystallization with triphenylphosphine oxide (TPPO) does not appear to yield better SHG efficiency in the α-methylbenzylamine substituted ethylene compound which has an extended hydrogen bonding network.

Keywords: Hydrogen bonding; Chirality; Second harmonic generation; Push–pull ethylene

1. Introduction

The design of π conjugated molecules substituted with suitable donor and acceptor groups for enhanced second-order non-linear optical (NLO) application has been the subject of much recent research [1,2]. Most studies of this nature have been focussed, thus far, on donor–acceptor aromatic systems [3,4]. The push–pull conjugated molecules are potentially useful for developing electro-optic switching in telecommunications, optical information processing, etc. These molecules are also important since they are atypical conjugated donor–acceptor systems and as such can serve as models for both experimental and theoretical understanding of NLO structure–property relationships. The optimal molecular parameters necessary for maximization of second harmonic generation (SHG) in the bulk, i.e., in crystals, may be derived through molecular and crystal engineering approaches. However, in general these parameters are subtle, less well understood and more difficult to control [5,6]. One of the well known approaches is to make use of the influence of hydrogen bonding on the geometry and crystal packing of organic solids. It has been shown [7] earlier that hydrogen bonding plays an important role in enhancing the SHG efficiency in a series of organic salts of dihydrogenphosphate and L-tartaric acid. Usually in donor–acceptor substituted compounds large ground state dipole moments of the molecules tend to favor centro-

* Corresponding author.

SSDI 0022-2860(95)09180-7

symmetric crystal structures by aligning in a head-to-tail fashion and thus destroying the net alignment necessary for SHG. The hydrogen bond energy is comparable to the dipolar interaction energy, E_μ and can, in some instances, bring about a favorable orientation of molecular dipoles in a solid, but despite careful planning it is difficult to predict a priori the molecular alignment and packing in crystals. Yet, there have been many successful crystal engineering attempts to design efficient SHG active molecules by exploiting the hydrogen bonding property of the attached functional groups or attaching a chiral handle (also having a hydrogen bond acceptor or donor) to the molecule [8]. Some examples of highly efficient compounds synthesized based on the above approach are *N*-4-nitrophenylprolinol (NPP), 2-methyl-4-nitro-*N*-methyl-aniline (MNMA), 2-*N*-(α-methylbenzylamino)-5-nitropyridine (MBA-NP), 2,4-dinitrophenyl-L-alanine methyl ester (MAP), 2-(*N*-prolinol)-5-nitropyridine (PNP), etc. Sometimes the influence of hydrogen bonding leads to pseudo-antiparallel orientations (also called pseudo-inversion dimers) resulting in an equilibrium structure which is nearly centrosymmetric and has the molecules in an unfavorable orientation [9–11] for SHG.

In this paper, we report the microscopic and bulk second-order non-linearities in some substituted ethylenes with varying donor or acceptor groups having, respectively, different electron donating or accepting ability. For bulk SHG we attempt to improve packing and molecular alignment by introducing groups that can form H-bonds (e.g., methylamino) or have a chiral center (like α-methylbenzylamine). α-Methylbenzylamine was chosen as it guarantees a non-centrosymmetric crystal structure, and has been shown to impart interesting packing characteristics suitable for phase matched SHG as in MBA-NP. We have used the hyper-Rayleigh scattering (HRS) technique [12–21] for measuring the microscopic second-order non-linearity (β) in these compounds. It is a direct technique for measuring $\langle\beta\rangle$ for molecules independent of solvent contribution. In order to understand the bulk non-linearity in these compounds, we have determined the crystal structures of two of them.

2. Experimental

2.1. Synthesis of polarized ethylenes

Compounds **1a–1h** (Fig. 1) were synthesized using literature procedures with certain modifications wherever necessary [22–25]. For the preparation of **1d**, R(+)-α-methylbenzylamine (0.605 g, 0.005 mol) in acetonitrile was added slowly to a stirred solution of **1b** (0.75 g, 0.005 mol) in acetonitrile (15 ml). The solution was refluxed for 24 h in the presence of catalytic amounts of *p*-toluene sulfonic acid. The concentrate was passed through a neutral alumina column and **1d** separated by using ethyl acetate/ethanol (8:2) as the eluent. The solid formed after evaporating the solvent was recrystallized from benzene. The product was characterized by NMR, IR and mass spectra. From the NMR peak intensities two isomers are found to exist in solution in 3:1 ratio. In one of the isomers (major) the α-methylbenzylamino group is cis to the nitro group and in the other (minor) it is trans. For **1d**, m.p. 152–153°C; ν (cm^{-1}), 2998(NH), 1578(NO_2); ^1H NMR, (δ in ppm) **NH**, 10.57(s,1H), 10.31(s,1H); $C_6\mathbf{H}_5$, 7.35(m,5H); $CHNO_2$, 6.54(s,1H), 6.46(s,1H); **NH**, 5.57(s,1H), 5.09(s,1H); **CH**Me, 4.63(q,1H); NCH_3, 3.03(s,3H); NCH_3, 2.70(dd,3H).

2.2. Absorption measurements

UV-Visible spectra of **1a–1h** were recorded in freshly prepared solutions in methanol in a Hitachi (U-3400) spectrometer.

2.3. SHG measurements

Bulk SHG was measured with respect to urea using the Kurtz and Perry [26] powder technique. The microscopic hyperpolarizabilities (β) in these compounds were measured by the HRS technique with 1064 nm radiation. The experimental setup is described in detail elsewhere [13].

2.4. Crystal structure determination

The three-dimensional intensity data for both **1d** and **1h** were collected on an Enraf–Nonius CAD-4 diffractometer. Structures were solved by direct

methods using SHELXS 86 and refined by the full matrix least squares method using SHELX 76 programs. The non-H atoms were refined anisotropically and the H-atoms were introduced at calculated positions but not refined. The refinement converged to an R factor of 0.061 and $R_w = 0.067$ for **1d** and $R = 0.031$ and $R_w = 0.034$ for **1h**. The relevant crystallographic data are presented in Tables 3–12 below for **1d** and **1h**. The anisotropic temperature factors and F_0/F_c values are available as supplementary material.

3. Results and discussion

3.1. UV-visible spectra of 1a–1h

The λ_{max} values of **1a–1h** are listed in Table 1. They exhibit an intense broad band around 330 nm due to an n–π^* transition with the ground state having varying π-character. Another low intensity band around 250 nm (spectra not shown) is also observed which originates from a high energy π–π^* transition. The optical activity of the compound **1d** was checked by recording the circular dichroism (CD) spectrum (spectrum not shown).

3.2. First hyperpolarizability (β) measurements

The first hyperpolarizability tensor of these molecules measured by the HRS method in methanol are listed in Table 1. We have also listed the ground state dipole moments (μ_g) for **1a–1h** at the AM1 [27] level with full geometry optimization. Quadratic hyperpolarizabilities were also

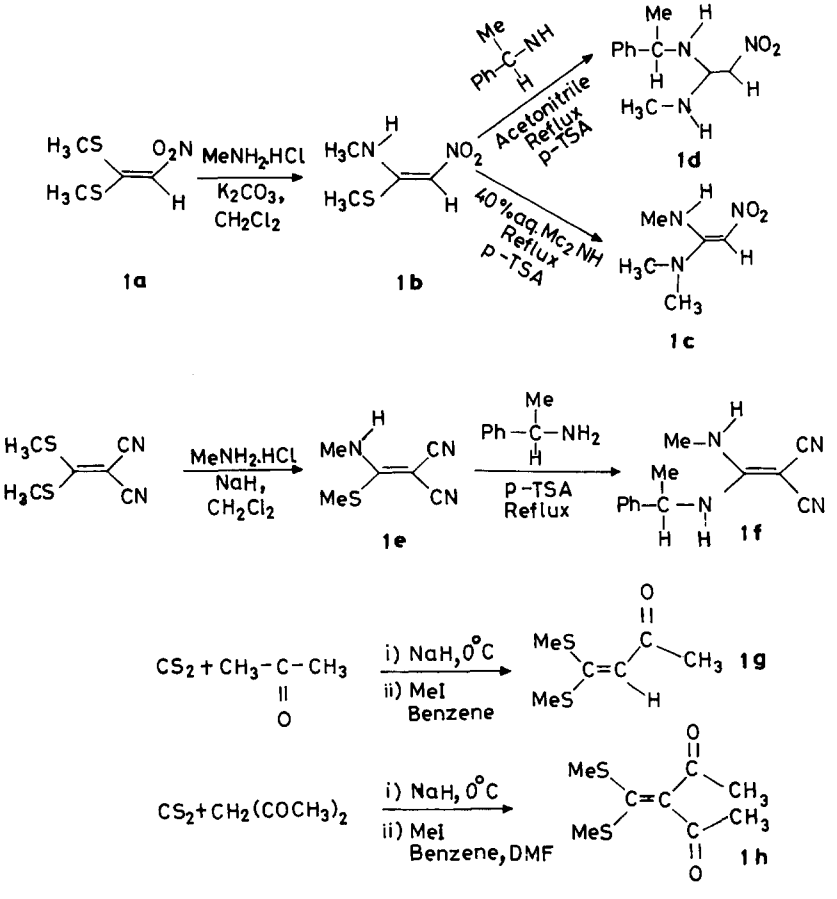

Fig. 1. Schematic representation of the synthetic procedures adopted for preparation of **1a–1h**.

Table 1
λ_{max} (nm) for **1a–1h** in methanol, their calculated ground state dipole moments (D) and lengths (Å) and measured quadratic hyperpolarizabilities ($\times 10^{-30}$ esu) in methanol and powder SHG efficiency with respect to urea (×U)

Compound	λ_{max}	μ_g	β_{HRS}	$\beta_{calc.}$	Powder SHG
1a	354.1	4.82	3.3	1.1	ND*
1b	352.3	6.28	4.3	1.4	ND
1c	335.7	6.43	5.2	1.9	ND
1d	345.1	6.81	7.6	2.1	0.5U
1e	293.8	5.89	2.3	0.9	0.5U
1f	292.6	7.05	4.2	1.4	0.2U
1g	380.6	2.42	1.8	0.8	ND
1h	319.4	3.17	2.1	0.9	0.5U

* ND, not detected.

computed at the AM1 level available in the MOPAC package using the finite field model [28] (Table 1). The trends in experimentally measured and theoretically calculated β values are similar. From our results for substituted ethylene compounds we note that for a fixed acceptor or donor the β value changes with increasing strength of the donor or acceptor groups. For example, in **1c** the presence of a $-NMe_2$ group instead of a –SMe group as in **1b** enhances β. Similarly in **1d** the –NHMeϕ group leads to a further improvement in β. Also a $-NO_2$ functional group is a better acceptor than either the –CN or –COMe group.

3.3. Solvent effects on β

From Table 1, we note that the experimental β value is much higher than the gas phase number calculated by semiempirical methods. We have measured β for all the compounds in four different solvents having different dielectric constants. They are listed in Table 2. In general, a number of different solute–solvent effects [29] can occur such as excited state effects [30], van der Waals interactions, dipolar interactions, hydrogen bonding and intermolecular charge transfer interactions [31]. We can approximate the first hyperpolarizability in solution as

$$\beta = \beta_g + \beta_{dip}(1 - g) + \beta_{hb} + (\beta_{solvent} - \beta_{hb}) f_s$$

where β_g is the hyperpolarizability of the molecules with no interaction at all (i.e., in the gas phase), β_{dip} is the hyperpolarizability produced by the dipolar interaction between the solute molecules, $\beta_{solvent}$ is the hyperpolarizability change produced by the solute–solvent interaction (e.g., van der Waals, dipolar, charge transfer), β_{hb} is the hydrogen bonding contribution to β, f_s is the volume fraction of the solvent and g is the well known Kirkwood factor [32] which describes a pairwise molecular correlation and $g < 1$. In carbon tetrachloride, since intermolecular hydrogen bonding is absent, the solvent effect results from dipole–dipole interaction and it increases as the dipole moment (or the electron donating power (σ) of the donor) of the molecule increases. In fact, the dipolar contribution to β i.e., β_{dip} can be approximated as the difference between the measured β in carbon tetrachloride and the calculated β i.e., the gas phase number. But in acetone, methanol and DMSO, both intramolecular and intermolecular hydrogen bonding are possible and as a result β in these three solvents is higher than in carbon tetrachloride.

Table 2
β (in units of 10^{-30} esu) for compounds **1a–1h** in different solvents

Compound	$\beta_{carbon\ tet.}$	$\beta_{acetone}$	$\beta_{methanol}$	β_{DMSO}
1a	2.4	2.7	3.3	3.1
1b	3.2	3.4	4.3	3.8
1c	4.1	4.2	5.2	4.6
1d	5.1	5.3	7.6	5.8
1e	1.1	1.3	2.3	1.7
1f	2.4	2.7	4.2	2.9
1g	0.9	1.1	1.8	1.3
1h	1.2	1.4	2.1	1.6

3.4. Powder SHG measurements

The powder SHG efficiencies are given in Table 1. At the molecular level none of the compounds has a center of inversion. However, only compounds **1d**, **1e**, **1f**, **1h** exhibit moderate SHG efficiencies. Except **1a**, all the compounds possess groups that can form, in principle, intramolecular hydrogen bonds. Compound **1b** has been proposed to have a structure in which the MeNH– group is involved in intramolecular hydrogen bonding with the nitro group [33–35]. We believe that the compounds **1a–1c** do not exhibit SHG due to a nearly

centrosymmetric structure in the solid state. Such an unfavorable structure is probably due to pairing of molecules in the crystal lattice in a head-to-tail fashion. Compound **1d** crystallizes in a non-centrosymmetric space group $P2_1$. However, this alone will not result in a very large SHG efficiency. **1e** has an efficiency 0.5 times that of urea whereas **1f** has an efficiency only 0.2 times that of urea. This decrease in efficiency in going from **1e** to **1f** may be due to the difference in the packing characteristics which are altered because of steric crowding in the latter. Between **1g** and **1h**, only **1h** exhibits a SHG efficiency. In order to investigate further, the crystal structures of **1d** and **1h** were determined.

3.5. Crystal structures of 1d and 1h

Single crystals of **1d** were obtained from a saturated solution of ethyl acetate/benzene (1 : 9). The compound **1d** crystallizes in the monoclinic space group $P2_1$. An ORTEP of the molecular structure is shown in Fig. 2 and the packing diagram in Fig. 3. The crystal data, observed bond distances, bond angles and torsion angles are listed in Tables 3, 4, 5 and 6, respectively. Final atomic positional parameters are given in Table 7. An idea about the extent of delocalization in **1d** can be obtained from the observed bond distances in Table 4. The C=C distance which is a measure of the charge transfer between the donor

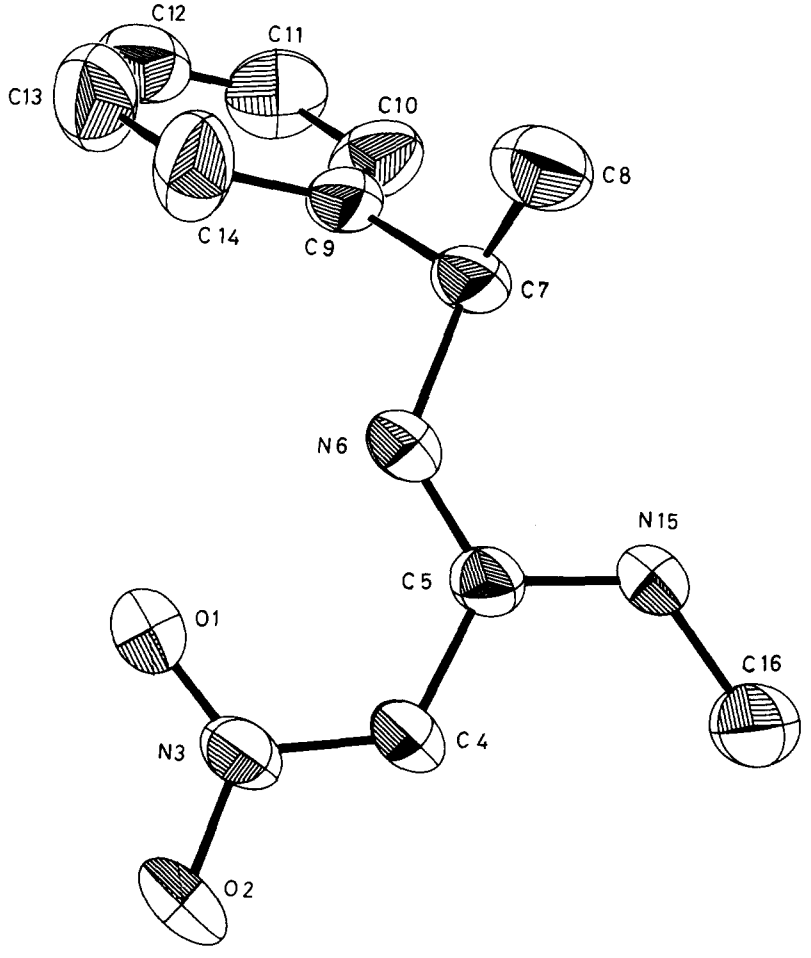

Fig. 2. Molecular structure of **1d**.

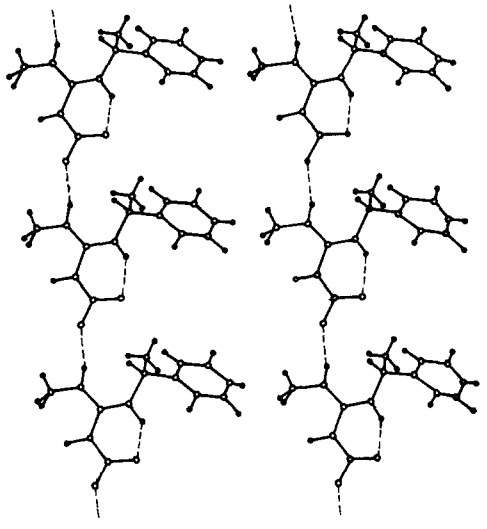

Fig. 3. Packing diagram of **1d** illustrating the intramolecular and intermolecular hydrogen bonding.

Table 3
Crystal data for **1d**

Formula	$C_{11}H_{15}N_3O_2$
Formula weight	221.3
Crystal size	0.3 × 0.15 × 0.1 mm^3
System, space group	Monoclinic, $P2_1$
a (Å°)	7.372(2)
b (Å)	6.959(1)
c (Å)	11.363(3)
β (deg)	95.98(2)
V (Å^3)	579.3
d_{calc} (g cm^{-3})	1.267
Z	2
$F(000)$	236.0
μ (Cu Kα) (cm^{-1})	0.711
Temp (°C)	19
Scan method	$w/2\theta$
Octants (coll.)	+8, +7, ±12
2θ range (deg)	120
Total reflections	1087
Unique reflections	920
Observed reflections	798 [$I > 2.5\sigma(I)$]
No. of parameters	146
R	0.061
R_w	0.067
GOF	0.68
Largest shift (esd)	0.05
Largest peak, e(Å)	0.16

Table 4
Selected bond distances (Å) for **1d**

O1–N3	1.251(5)	C7–C8	1.519(1)
O2–N3	1.274(4)	C7–C9	1.505(8)
N3–C4	1.347(5)	C9–C10	1.357(7)
C4–C5	1.425(5)	C9–C14	1.397(8)
C5–N6	1.292(6)	C10–C11	1.405(10)
C5–N15	1.346(5)	C11–C12	1.368(10)
N6–C7	1.487(5)	C12–C13	1.373(13)
N6–H6	0.906(51)	C13–C14	1.349(10)
N15–H1	0.565(45)	N1–C16	1.442(6)

and the acceptor groups is 1.425(5) Å. This is very long compared to the corresponding distance of 1.333(6) Å in unsubstituted ethylene. Further, the extent of delocalization is also shown by a marked decrease [36] in the C–N donor distances (1.292(5) Å for the cis and 1.346(5) Å for the trans nitrogens, respectively) and the C–N (acceptor) distance of 1.347(5) Å due to the participation of the nitrogen lone pair in the resonance. It is surprising that the shortest C–N (donor) distance is observed for the C–N in the α-methylbenzylamine moiety which is cis with respect to the nitro group (torsion angle, 0.73(8)°). The methylamino group is almost trans to the nitro group (torsion angle, −179.7(6)°), i.e., in a conformation in which the nitrogen is in the plane of the C=C double bond and the nitro group. Both the electron donating nitrogen atoms are in the same plane as the C=C double bond as indicated by the angles about the nitrogen atoms which are 359.8° and 359.6°, respectively.

The extent of conjugation in a molecule is governed by the relative importance of the intramolecular steric interactions between the

Table 5
Selected bond angles (°) for **1d**

O1–N3–O2	119.8(3)	O2–N3–C4	117.4(3)
O1–N3–C4	122.6(3)	N3–C4–C5	123.3(4)
C4–C5–N15	118.1(4)	C4–C5–N6	121.4(4)
N6–C5–N15	120.4(4)	C5–N6–C7	127.0(3)
N6–C7–C9	109.0(3)	N6–C7–C8	109.6(4)
C8–C7–C9	113.4(5)	C7–C9–C14	121.1(5)
C7–C9–C10	121.4(4)	C10–C9–C14	117.3(5)
C9–C10–C11	121.1(6)	C10–C11–C12	120.0(7)
C11–C12–C13	118.7(6)	C12–C13–C14	120.9(7)
C9–C14–C13	121.7(7)	C5–N15–C16	124.4(3)

Table 6
Torsional angles (°) of non-hydrogen atoms for **1d**

O2–N3–C4–C5	−174.7(5)	O1–N3–C4–C5	3.1(8)
N3–C4–C5–C6	0.7(8)	N3–C4–C5–N15	−179.8(5)
C4–C5–N15–C16	5.5(18)	C4–C5–N6–C7	178.4(5)
N6–C5–N15–C16	−174.9(5)	N15–C5–N6–C7	−1.0(8)
C5–N6–C7–C8	−85.1(7)	C5–N6–C7–C9	149.9(5)
N6–C7–C9–C10	114.1(7)	C8–C7–C9–C14	−64.2(7)
C7–C9–C14–C13	0.0(1)	C14–C9–C10–C11	0.0(1)
C9–C10–C11–C12	0.0(8)	C10–C11–C12–C13	0.0(1)
C11–C12–C13–C14	0.0(9)	C12–C13–C14–C9	0.0(1)

substituents on the double bond and the loss of π–electron energy due to the rotation about the double bond [37,38]. These two factors together determine the minimum energy conformation of the molecule. The steric interaction is minimum in the 90° twisted conformation. In conjugated olefins, in the absence of steric forces, the planar conformation is preferred. However, when both the forces are operating there is a twist about the C=C bond, the magnitude of which depends upon the relative importance of these two factors. This twist angle is small (2.31°) in **1d** and, as a result, extended delocalization of electrons is possible.

Single crystals of **1h** were obtained from a saturated solution of methanol. The ORTEP diagram of **1h** is displayed in Fig. 4 and the unit cell packing diagram in Fig. 5. The crystal structure data are listed in Table 8. Selected bond distances, bond angles and dihedral angles for **1h** are given in Tables 9, 10 and 11, respectively. The atomic coordinates are listed in Table 12. The same structure has been reported recently by Zou et al. [39] but no details have been provided. The observed C=C bond distance in this molecule is comparable to that in ethylene indicating that the extent of delocalization is insignificant. This may be due to the following factors: (1) the molecule is non-planar with the (S1C1C2C4) dihedral angle being 13.5° which hinders delocalization; (2) the $-COCH_3$ group as an acceptor and $-SCH_3$ as a donor are poor and are unable to push and pull electrons effectively across the ethylene backbone, respectively. The reduced charge-transfer interaction may also arise from increased steric interactions between the various substituents. Steric interaction could be minimized by rotation about the C=C bond. Such a situation is, in fact, observed in dimethylaminoethylene-malonate [40,41], where, one of the methyoxy-carbonyl groups is pushed out of the plane and the rest of the molecule is planar, with delocalization of electrons between Me_2N- and the carbonyl groups. The non-bonded distance S1–C4 (3.068 Å) in **1h** is less than the sum of the van der Waals radii (3.500 Å) of the two atoms. This is an indication of the steric interference in this molecule in spite of the twist about the C=C bond. The presence of the two carbomethoxy groups leads to various possible conformations (for a detailed discussion on this see Ref. [27]). However, the EE form of **1h** is less likely because of the strong repulsion expected between two parallel dipoles.

Table 7
Atomic coordinates for **1d**

Atom	*X/a*	*Y/b*	*Z/c*
O1	−0.753(4)	−0.111(3)	−0.641(3)
O2	−0.584(4)	−0.166(10)	−0.474(3)
N3	−0.740(4)	−0.135(9)	−0.531(3)
C4	−0.886(5)	−0.135(9)	−0.469(4)
C5	−1.069(5)	−0.118(10)	−0.522(4)
N6	−1.106(5)	−0.103(9)	−0.636(3)
C7	−1.290(5)	−0.089(12)	−0.703(4)
C8	−1.367(7)	−0.289(12)	−0.727(5)
C9	−1.276(6)	0.026(11)	−0.813(4)
C10	−1.378(9)	0.186(13)	−0.837(5)
C11	−1.368(9)	0.290(14)	−0.942(6)
C12	−1.254(9)	0.231(15)	−1.023(5)
C13	−1.150(9)	0.069(16)	−0.998(5)
C14	−1.160(8)	−0.030(14)	−0.897(5)
N15	−1.204(4)	−0.120(10)	−0.451(3)
C16	−1.176(6)	−0.121(13)	−0.234(4)

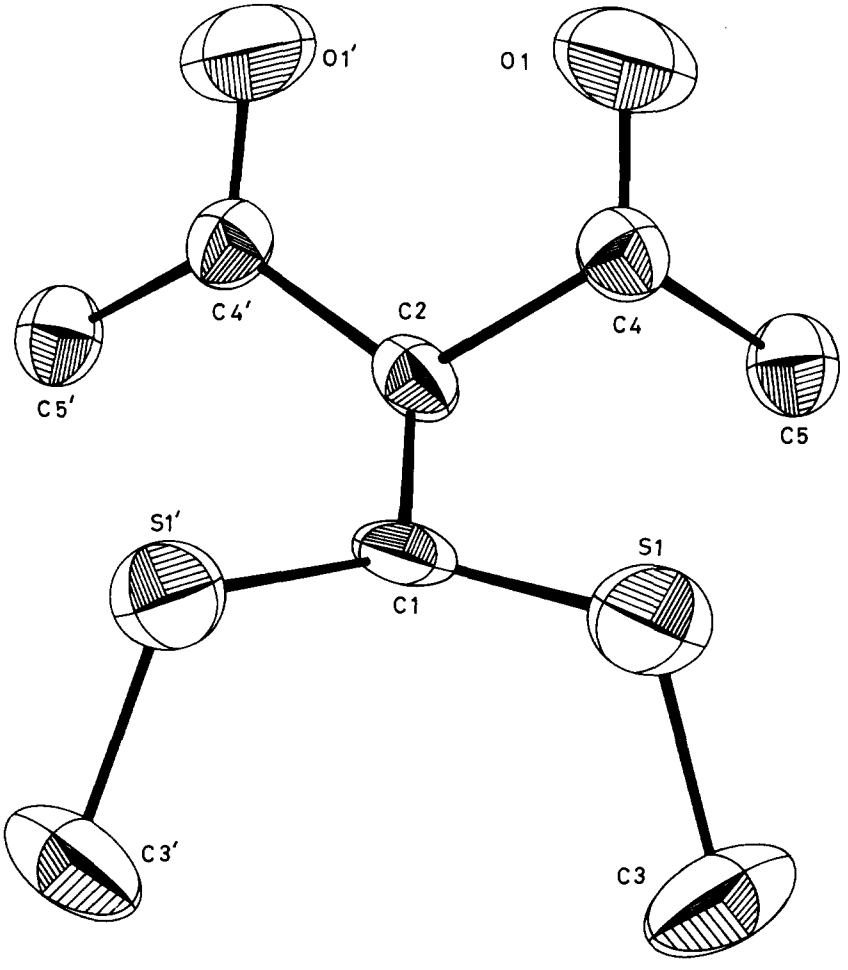

Fig. 4. Molecular structure of **1h**.

3.6. Hydrogen bonding network

Both intramolecular and intermolecular hydrogen bonds [42] are observed in **1d** resulting in an extended hydrogen bond network (Fig. 3). The intramolecular hydrogen bond is formed between the –NH of the α-methylbenzylamine and the nitro group (distances N6–O1, 2.609(4) Å and H6–O1, 1.838(5) Å, angle N6–H6–O1, 141.0(4)°). The intermolecular hydrogen bond is observed between the –NH of the methylamino group (which is trans to the $-NO_2$ group) and the oxygen of the NO_2 group from the neighbouring molecule (distances N15–O2, 2.806(4) Å and H15–O2, 1.966(5) Å and angle N15–H15–O2, 163(4)°). The intramolecular hydrogen bonding results in a non-polar structure while the intermolecular hydrogen bonds extend to a one-dimensional network. Assuming the charge transfer (CT) axis of the molecule to coincide with the C=C axis, we have calculated the angle between the CT axis from the crystallographic '*b*' axis (the only C_2 axis of the molecule coincides with the '*b*' axis) as 77.29° (the ideal angle for $P2_1$ symmetry being 54.7° [43,44]). In other words, the CT axis in **1d** is almost perpendicular to the '*b*' axis. This leads to a orientation of the molecules in the crystal lattice that is very unfavorable for efficient frequency doubling.

To improve the SHG efficiency we have attempted to cocrystallize **1d** with triphenylphosphine oxide

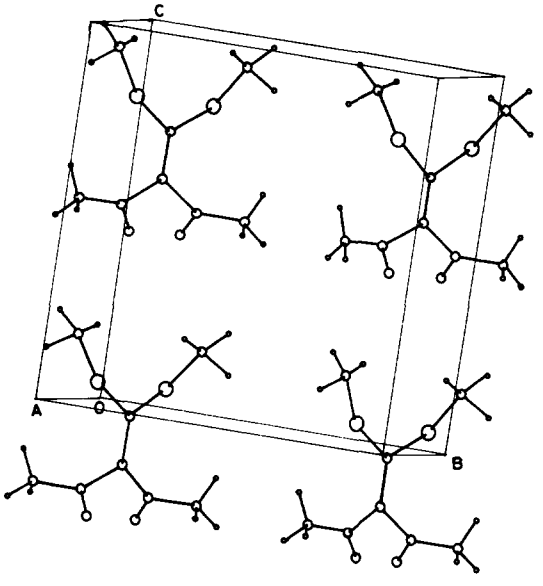

Fig. 5. Packing diagram of **1h** molecules viewed through the *x*-axis.

Table 8
Crystal structure data for **1h**

Formula	$C_8H_{12}O_2S_2$
Formula weight	204.3
Crystal size	0.25 × 0.15 × 0.15 mm^3
Space group	$p2_12_12$
a (Å)	7.966(1)
b (Å)	8.048(1)
c (Å)	8.088(1)
V (Å^3)	518.5(1)
d_{calc} (g cm^{-3})	1.3085
Z	2
F(000)	216.0
μ (Mo Kα) (cm^{-1})	4.547
Temp. (°C)	19
Scan method	$w/2\theta$
Octants (coll.)	+10, +10, +10
2θ range (deg)	50
Total reflections	718
Unique reflections	687
Observed reflections	649 [$I > 2.5\sigma(I)$]
No of parameters	61
R	0.032
R_w	0.034
GOF	0.551
Largest shift (esd)	0.009
Largest peak, *e*(Å)	0.21

Table 9
Selected bond distances (Å) for **1h**

C1–C2	1.355(3)
C1–S1	1.755(1)
C2–C4	1.504(2)
C3–S1	1.800(3)
C4–C5	1.491(3)
C4′–O1′	1.198(3)

Table 10
Selected bond angles (°) for **1h**

S1–C1–S1′	121.6(0)
C2–C1–S1	119.2(1)
C1–C2–C4	123.3(1)
C4–C2–C4′	113.3(2)
C2–C4–O1	119.3(2)
C2–C4–C5	117.4(1)
C5′–C4′–O1′	122.9(3)
C1–S1–C3	103.8(1)

Table 11
Torsional angles (°) for **1h**

S1–C1–S1′–C5	47.0(1)
C2–C1–S1–S3	−132.9(1)
S1–C1–C2–C4	13.5(2)
S1′–C1–C2–C4	−166.4(1)
C1–C2–C4–C5	70.5(2)
C1–C2–C4–O1	−115.6(2)
C4′–C2–C4–O1′	64.4(2)

Table 12
Atomic coordinates for **1h**

Atom	*X*/*a*	*Y*/*b*	*Z*/*c*
C1	0.0000	0.5000	−0.0554
C2	0.0000	0.5000	−0.2230
C3	0.0494(4)	0.2762(4)	0.2050(4)
C4	0.1070(3)	0.3853(2)	−0.3852(2)
C5	0.0615(3)	0.2053(3)	−0.3264(3)
S1	0.1600(1)	0.3942(1)	0.0504(1)
O1	0.2145(3)	0.4427(3)	−0.4177(3)

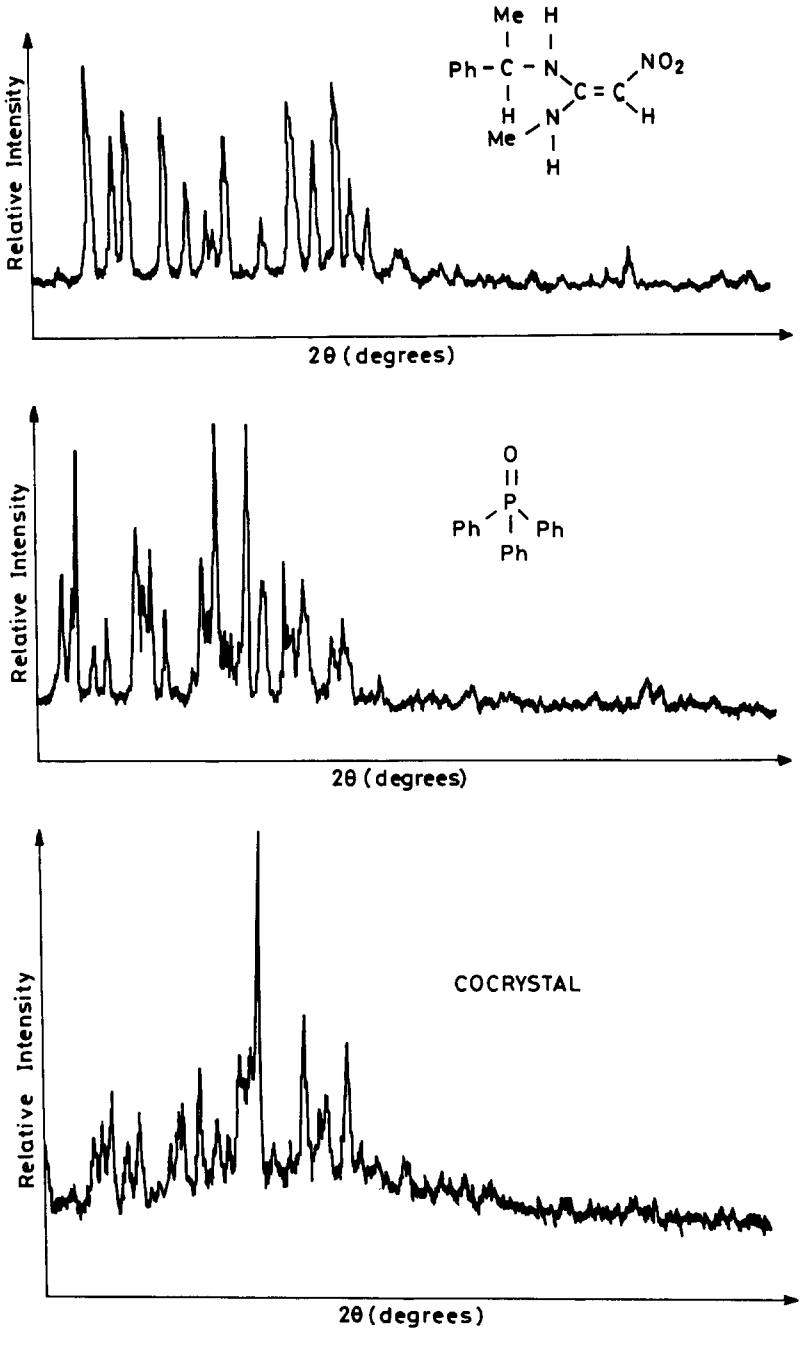

Fig. 6. X-ray powder diffraction patterns for **1d**, TPPO and their 1 : 1 complex.

(TPPO). It has been demonstrated by Etter [45] that many organic materials crystallize readily as large crystals having sharp edges and well defined crystal faces when they are cocrystallized with TPPO. Etter has also shown that complexation with TPPO is a new method for transforming compounds into better quality crystals. The factors responsible for the influence of TPPO on crystal growth are two fold; (i) the strong hydrogen bond between the molecule and TPPO imparts a partially

ionic character, and (ii) the bulky shape of the TPPO molecules inhibits the formation of lamellar structures that cause crystals to fracture easily and grow as thin plates. The complexation was carried out by dissolving equimolar quantites of **1d** and TPPO, in a mixture of ethyl acetate/toluene and the solvent was evaporated slowly at room temperature. The complex formation was confirmed from the melting point, IR, NMR data and X-ray powder patterns. In spite of repeated attempts, good quality cocrystals could not be obtained for the structure determination. However the X-ray powder pattern of the complex along with that of TPPO and **1d** are given in Fig. 6. The powder pattern confirms the formation of the 1 : 1 complex; m.p. of the complex 115°C; ^{1}H NMR data (δ in ppm) 10.57 (s, 1H), 10.25 (s, 1H), 6.53 (s, 1H) 4.97 (s, 1H), 4.62 (d, $J = 6.2$, 1H), 3.01 (s, 3H), 2.65 (d, 2H).

The SHG efficiency of the complex is only 0.1 × U. The reduction in the efficiency perhaps results from the disruption of the one-dimensional hydrogen bonding network in **1d**. However, strong intramolecular hydrogen bonding is likely since the complex is highly stable.

Conclusion

In this paper we have critically examined the influence of chirality as well as hydrogen bonding on the microscopic and macroscopic second-order non-linearities in some push–pull ethylenes. Intermolecular hydrogen bonding in the solid state with another molecule or in solution with solvent molecules seems to enhance the first hyperpolarizability in these systems. The presence of a chiral group in the molecule always guarantees a non-zero macroscopic second-order susceptibility. Optimization of $\chi^{(2)}$ by cocrystallization with TPPO turns out to be less controlled since a trade off between the intermolecular and intramolecular hydrogen bonding reduces the frequency doubling efficiency. Longer polyenes with chiral donor or acceptor groups and an extended intermolecular hydrogen bonding network hold much promise for efficient frequency doubling materials in the future.

Acknowledgements

We thank Dr S. Rajappa for many helpful discussions regarding the synthesis of the push–pull ethylenes. The laser was purchased with a grant from the Department of Science and Technology, Government of India. Generous financial support from the director, Indian Institute of Science for our research is gratefully acknowledged.

References

[1] R.J. Tweig and K. Jain, in D.J. Williams (Ed.), Nonlinear optical properties of organic and polymeric materials, ACS Symp. Ser. 233, American Chemical Society, Washington, DC, 1983, p. 27.
[2] S.R. Marder, J.E. Sohn and G.D. Stucky (Eds.), Materials for nonlinear optics: chemical Perspectives, ACS Symp. Ser. 455, American Chemical Society, Washington, DC, 1991.
[3] P.N. Prasad and D.J. Williams, Introduction to Nonlinear Optical Effects in Molecules and Polymers, John Wiley & Sons Inc., New York, 1991.
[4] D.S. Chemla and J. Zyss (Eds.), Nonlinear Optical Properties of Organic Molecules and Crystals, Academic Press, New York, 1987.
[5] G. Desiraju, in Crystal Engineering: The Design of Organic Solids, Material Science Monographs, Vol. 54, 1989, Elsevier, Amsterdam.
[6] J. Zyss and G. Tsoucaris, Mol. Cryst. Liq. Cryst., 137 (1986) 303.
[7] J. Zyss, J.F. Nicoud and M.J. Coquillay, Chem. Phys., 81 (1984) 4160.
[8] A.I. Kitaigorodsky, Molecules and Molecular Crystals, Academic Press, New York, 1987.
[9] R.T. Bailey, F.R. Cruickshank, S.M.G. Guthrie, B.J. Mcardle, D. Pugh, E.A. Shepherd, J.N. Sherwood, C.S. Yoon, R. Kashyap, B.K. Nayar and K.I. White, in R.A. Hann and D. Bloor (Eds.), Organic Materials for Nonlinear Optics, The Royal Society of Chemistry, London, 1989, p. 129.
[10] K.D. Singer, Ph.D. Dissertation, University of Pennsylvania, 1981.
[11] J.F. Nicoud and R.J. Twieg, in D.S. Chemla and J. Zyss (Eds.), Nonlinear Optical Properties of Organic Molecules and Crystals, Academic Press, New York, 1987, p. 227.
[12] P.C. Ray and P.K. Das, J. Phys. Chem., 99 (1995) 17891.
[13] K. Clays and A. Persoons, Phys. Rev. Lett., 66 (1991) 2980.
[14] K. Clays and A. Persoons, Rev. Sci. Instrum., 63 (1992) 3285.
[15] W.M. Laidlaw, R.G. Denning, T. Verbiest, E. Chauchard and A. Persoons, Nature, 363 (1993) 58.
[16] K. Clays, E. Hendricks, M. Triest, T. Verbiest, A. Persoons, C. Dehu and J.L. Bredas, Science, 262 (1993) 26.

[17] J. Zyss, T. Chauvan, C. Dhenaut and I. Ledoux, Chem. Phys., 177 (1993) 281.
[18] J. Zyss, C. Dhenaut, T. Chauvan and I. Ledoux, Chem. Phys. Lett., 206 (1993) 409.
[19] J. Zyss and I. Ledoux, Chem. Rev., 94 (1994) 77.
[20] R.W. Terhune, P.D. Maker and C.M. Savage, Phys. Rev. Lett., 17 (1965) 681.
[21] R. Bersohn, Y.H. Pao and H.L. Frisch, J. Chem. Phys., 45 (1966) 3184.
[22] R. Gompper and H. Schaffer, Chem. Ber., 100 (1967) 591.
[23] H. Junjappa, personal communication, 1991.
[24] Y. Shovo and I. Belsky, Tetrahedron, 25 (1969) 4649.
[25] K. Mohonalingam, P.K. Das and S. Rajappa, Spectrochim. Acta Part A, 48 (1992) 1647.
[26] S.K. Kurtz and T.T. Perry, J. Appl. Phys., 39 (1968) 3798.
[27] M.J.S. Dewar, G.E. Zeobisch, F.E. Healy and J.J.P. Stewart, J. Am. Chem. Soc., 107 (1985) 3902.
[28] H.A. Kurtz, J.J.P. Stewart and K.M. Dieter, J. Comput. Chem., 11 (1990) 82.
[29] J. Zyss and I. Ledoux, Chem. Phys., 73 (1982) 203.
[30] A. Schweig, Mol. Phys., 15 (1968) 1.
[31] B.F. Levine and C.G. Bethea, J. Chem. Phys., 65 (1976) 2439.
[32] N.E. Hill, W.E. Vaughan, A.H. Price and M. Davies, Dielectric Properties and Molecular Behaviour, Van Nostrand, Princeton, NJ, 1969.
[33] M.S. Paley, J.M. Harris, H. Looser, J.C. Baumert, G.C. Bjorklund, D. Jundt and R.J. Tweig, J. Org. Chem., 54 (1989) 3774.
[34] W. Schuddeboom, B. Krijnen, J.W. Verhoeven, E.G.J. Staring, G.L.J.A. Rikken and H. Oevering, Chem. Phys. Lett., 179 (1991) 73.
[35] Y. Goto, A. Hayashi, Y. Kimura and M. Nakayama, J. Cryst. Growth, 108 (1991) 688.
[36] S. Rajappa, B.M. Bhawal, A.R.A.S. Deshmukh, S.G. Manjunatha and J. Chandrasekhar, J. Chem. Soc. Chem. Commun., (1989) 1729.
[37] J.L. Oudar, D.S. Chemla and J. Jerphagnon, Phys. Rev. B, 12 (1975) 4534.
[38] M. Berzoukas, D. Josse, P. Fremaux, J. Zyss, J.F. Nicoud and J.O. Morley, J. Opt. Soc. Am. B, 4 (1987) 977.
[39] Y. Zou, J. Feng, J. Li and C. Ye, Synthetic Met., 71 (1995) 1743.
[40] U. Shmueli, H. Shanan-Atidi, H. Horwitz and Y. Shovo, J. Chem. Soc. Perkin Trans. II, (1973) 657.
[41] T.R. Lynch, I.P. Mellor and S.C. Nyburg, Acta Crystallogr., 27 (1971) 1948.
[42] J.M. Halbout, S. Blit and C.L. Tang, J. Quantum Electron., QE-17 (1981) 513.
[43] M.C. Etter and P.W. Baures, J. Am. Chem. Soc., 110 (1988) 639.
[44] M.C. Etter, Acc. Chem. Res., 23 (1990) 120.
[45] M.C. Etter, J. Phys. Chem., 95 (1991) 4601.